

# Interendothelial Junctions in Normal Human Schlemm's Canal Respond to Changes in Pressure

Wen Ye,\* Haiyan Gong,\* Arthur Sit,† Mark Johnson,† and Thomas F. Freddo\*

**Purpose.** To determine if changes in the structure and complexity of junctions between endothelial cells lining Schlemm's canal (SC) occur in normal human eyes with changes in perfusion pressure.

**Methods.** Twelve normal human eyes were either perfusion-fixed (at 15 or 45 mm Hg) or immersion-fixed (0 mm Hg) in modified Karnovsky's fluid. Outflow facility was measured continually during the perfusion fixation. The intercellular junctions of the endothelial cells of SC were ultrastructurally examined in thin sections, including serial sections and freeze-fracture replicas. Morphometric data on the number of junctional strands per total length of tight junction were documented and categorized by the number of strands (one, two, or three or more). The length of endothelial cell overlap was measured on thin sections.

**Results.** In freeze-fracture replicas, perfusion-fixed eyes demonstrated less complex junctions. At 15 mm Hg, 18.06% of the total junctional length was represented by three or more strands; at 45 mm Hg, this percentage decreased to 8.59%. In immersion-fixed eyes, 24.17% of the total junctional length was represented by three or more strands. These differences were statistically significant ( $P < 0.0012$ ). In sections, the amount of endothelial cell overlap, and thus the length of paracellular pathway, was reduced in perfusion-fixed versus immersion-fixed eyes ( $P < 0.02$ ). Extensive serial sectioning demonstrated that giant vacuoles were formed, either by individual endothelial cells or by two or more adjacent endothelial cells.

**Conclusions.** When compared with specimens fixed at zero pressure, overlap between endothelial cells of SC is reduced significantly when this cell layer is under conditions of flow similar to those encountered in vivo. The tight junctions between cells of the inner wall of SC become less complex with increasing pressure. Our data suggest that the paracellular pathway into SC in the normal eye is sensitive to modulation within a range of physiologically relevant pressures. Invest Ophthalmol Vis Sci. 1997;38:2460-2468.

The relative contributions of transcellular and paracellular pathways for transit of aqueous humor across the inner wall of Schlemm's canal (SC) are uncertain. When eyes are fixed at pressure, the inner wall of SC contains giant vacuoles protruding into the canal.<sup>1</sup> Associated with these giant vacuoles, but also occurring in nonvacuolated areas of the inner wall, are

small pores passing through the inner wall.<sup>1-3</sup> In a scanning electron microscopic study of the inner-wall endothelium of SC, Bill and Svedbergh<sup>4</sup> found that these pores could account for only a small fraction (perhaps 10%) of the total aqueous outflow resistance; for this reason, the inner wall of SC has been thought to be of only minor importance in determining outflow facility.

Epstein and Rohen's<sup>5</sup> study prompted reassessment of this issue. Using cationized ferritin perfusion, they reported that openings or lacunae with tunnel-like channels could occur between the cells, possibly augmenting paracellular flow. More recent studies have suggested that the pores found in the inner wall of SC may be either transcellular or paracellular, focusing new interest on the paracellular pathway between endothelial cells in the inner wall.<sup>6</sup> If paracellu-

From the \*Eye Pathology Laboratory, Boston University School of Medicine, Massachusetts, and the †Fluid Mechanics Laboratory, Massachusetts Institute of Technology, Cambridge, Massachusetts.

Supported by NIH grant #EY-09699, National Glaucoma Research, a program of the American Health Assistance Foundation, and by unrestricted departmental grants from Research to Prevent Blindness, Inc., The Massachusetts Lions Eye Research Fund, Inc. to Boston University, and to AS from The Natural Sciences and Engineering Research Council of Canada. Submitted for publication February 20, 1997; revised June 16, 1997; accepted July 8, 1997.

Proprietary interest category: N.

Reprint requests: Thomas F. Freddo, Eye Pathology Lab L-905, Boston University School of Medicine, 80 E. Concord Street, Boston, MA 02118.

lar flow accounts for a larger fraction of flow across the endothelium of SC than previously suspected, there must be accompanying changes in the tight junctions between adjacent cells.

In 1981, Raviola and Raviola<sup>7</sup> and Okinami<sup>8</sup> separately studied the structure of the intercellular junctions between the inner wall of SC in monkey eyes by freeze-fracture electron microscopy. The endothelial cells of the canal were seen to be joined by a form of tight junction in which the usual branching and anastomosing pattern of tight junctional strands was not observed. Instead, a much looser arrangement of strands containing intrajunctional openings (termed slit-pores) was found. Based on calculations using morphometric data obtained from immersion-fixed eyes, the Raviolas<sup>7</sup> also concluded that only a small fraction of aqueous humor outflow passes through these slit-pores. Recently, using the same technique as the Raviolas,<sup>7</sup> Bhatt et al<sup>9</sup> studied the intercellular junctions of SC endothelial cells in normal human eyes. They found that the intercellular junctions of these cells were similar but more complex than those found in monkey eyes, suggesting lower paracellular permeability.

All these freeze-fracture studies were performed on tissues fixed by immersion rather than under conditions of flow. Under conditions of zero flow, one rarely finds giant vacuoles in the inner wall. The structure of the inner wall of SC differs in specimens fixed by immersion fixation compared with perfusion fixation.<sup>10-14</sup> With such large differences in the behavior of the inner wall under conditions of flow versus no flow, it is reasonable to ask whether more subtle changes of physiological significance might also occur in the intercellular junctions between these cells when flow and no flow conditions are compared. In several tissues, tight junctions are known to vary their complexity in response to changing physiological conditions; certain of these changes have been found to be regulatory.<sup>15</sup> In our study, we used freeze-fracture to investigate whether changes in structure and complexity of the junctions between endothelial cells lining SC would occur in normal human eyes with changes in perfusion pressure.

## MATERIALS AND METHODS

Twelve eye bank eyes from donors with no known history of eye disease (ages 61 to 89 years) were obtained from National Disease Research Interchange within 24 hours after death. Donor eyes were used in accordance with the Declaration of Helsinki. Each eye was confirmed to be grossly normal by examination under a dissecting microscope.

Four pairs of eyes were perfusion-fixed, one at a constant pressure of 15 mm Hg and the other at a

constant pressure of 45 mm Hg. The remaining four eyes were immersion-fixed (0 mm Hg) for 3 hours at room temperature.

Each eye to be perfused was placed in a beaker and covered with saline, and then the beaker was placed into a water bath (34°C). A 25-gauge perfusion needle was inserted through the cornea, placing the tip into the posterior chamber of the eye, and a second 25-gauge exchange needle was then inserted through the cornea with the tip placed into the anterior chamber. The line from the exchange needle led to a waste reservoir and was initially clamped off.

A baseline outflow facility was measured at 15 or 45 mm Hg. The perfusion fluid used to obtain a baseline facility was Dulbecco's phosphate-buffered saline (Life Technologies, Grand Island, NY) with 5.5 mM glucose added, prefiltered through a 0.2-mm filter (cellulose acetate; Costar Scientific, Cambridge, MA). Flow into the eye was controlled using a computer-controlled syringe pump (model 22; Harvard Apparatus, South Natick, MA). Signals from the pressure transducers (Microswitch, 142PC05G; Brownell, Woburn, MA) were digitized using a MacADIOS-8ain A/D converter (GW Instruments, Somerville, MA) and fed into an Macintosh SE computer (Apple Computers, Cupertino, CA) for data acquisition and control. The control algorithm is described in detail by Whale et al.<sup>16</sup> Outflow facility was calculated as the ratio of the steady-state flow rate (usually reached in 30 minutes) to intraocular pressure.

After measurement of the baseline facility, the eyes were exchanged with fixative (2% paraformaldehyde, 2.5% glutaraldehyde in phosphate buffer, pH 7.3) and then fixed at the perfusion pressure. This was performed by placing the fixative-containing reservoir at a height 2 cm H<sub>2</sub>O above the fixation pressure, and placing the waste reservoir at a height 2 cm H<sub>2</sub>O below the fixation pressure. This protocol ensured that the average pressure in the eye was never >2 cm H<sub>2</sub>O away from the fixation pressure. Both reservoir lines were then opened to allow rapid exchange of the anterior chamber. Approximately 2 ml of fluid had to be exchanged to flush the anterior chamber and the fluid lines. A small amount (approximately 10 mg/100 ml of fixative) of fluorescein sodium salt (Sigma Chemical, St. Louis, MO) was added to help visualize the fixative and ensure that the anterior chamber was well exchanged. After the anterior chamber exchange, the eyes were perfused from the syringe pumps at the fixation pressure, and outflow facility was again measured.

The four eyes to be immersion-fixed were opened at the equator and then immersed in the same fixative solution as used for the perfusion fixation (2% paraformaldehyde, 2.5% glutaraldehyde in phosphate buffer, pH 7.3) for 3 hours at room temperature. The

perfusion-fixed eyes were opened at the equator after perfusion. The lens was gently removed from all eyes, and the anterior segment of each eye was cut radially into small wedges. At least two quadrants per eye were examined to reduce the influence of regional variability on resulting data.

### Freeze Fracture

The tissue wedges from each eye were embedded in 7% agar, and 190- $\mu\text{m}$  chopper sections were cut with a Smith-Farquhar tissue chopper (DuPont Co., Wilmington, DE). Some tissue-chopper sections were trimmed to contain only trabecular meshwork, SC, and a narrow strip of sclera. To facilitate the identification of the endothelium of the canal in freeze-fracture replicas, the lumen of the canal was carefully filled with homologous iris pigment, as described previously.<sup>7,9</sup>

The specimens were mounted on a double replica stage and fractured and replicated in a Balzer freeze-fracturing unit (BAF-301; Balzer High Vacuum, Santa Ana, CA) at  $-115^{\circ}\text{C}$  and  $10^{-7}$  torr. The replicated specimens were left overnight in methanol at room temperature to solubilize lipids, and then were digested in 5% sodium hypochlorite containing 10% to 15% potassium hydroxide. The replicas were rinsed in distilled water several times and then floated onto copper Gilder grids (Electron Microscopy Sciences, Ft. Washington, PA). The replicas were examined in a Philips 300 transmission electron microscope (Eindhoven, The Netherlands).

### Thin Sections

Some chopper sections were postfixated for 2 hours at  $4^{\circ}\text{C}$  in 1% osmium tetroxide and 1.5% potassium ferrocyanide in distilled water, dehydrated, and embedded in an Epon-Araldite mixture. The plane of section was first determined from thick sections in which orientation could be assessed. By trimming down these blocks to retain the proper orientation (once established), thin sections were cut and stained with uranyl acetate and lead citrate. Micrographs were taken on a Philips 300 transmission electron microscope. At least six sections per eye were examined. Extensive serial sections were cut in two perfusion-fixed eyes.

### Morphometry

**Freeze Fracture.** At least 14 replicas were examined per eye. Replicas averaged  $0.5\text{ mm}^2$  in area. All the junctions of the inner-wall endothelium of SC encountered were photographed at an original magnification of  $\times 20,000$  and enlarged to  $\times 54,000$  for measurement. The percentage of the total junctional length represented by one, two, or three or more strands was recorded. Junctional length was measured along

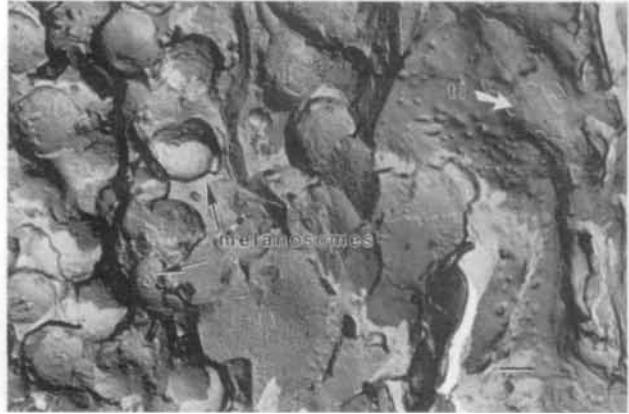


**FIGURE 1.** The lumen of Schlemm's canal was located by identifying the melanosomes that had been inserted into the canal before freezing. The melanosomes gave a distinct globular appearance (arrows). The inner-wall endothelial cells were joined by tight junctions (tj; arrow). Magnification scale bar =  $0.5\ \mu\text{m}$ .

a straight line parallel to the long axis of the junction on each micrograph. At least  $100\ \mu\text{m}$  of junctional length was measured per eye. Statistical analysis involving two groups used the Student's *t*-test to determine statistical significance. Data analysis involving two parameters (fixation pressure against total length of junctional strands) used a linear regression employing a two-sided Student's *t*-test to determine statistical significance of the slope (SYSTAT 5 for Macintosh, Evanston, IL).

**Thin Sections.** All the junctions of the inner-wall endothelium of SC encountered were photographed at an original magnification of  $\times 3300$  and enlarged to  $\times 8844$  for measurement. At least 100 interendothelial clefts from each eye were measured for the amount of cell overlap. Statistical analysis involving two groups (paired and unpaired comparison) used the Student's *t*-test to determine statistical significance.

## RESULTS

### Freeze Fracture

Schlemm's canal endothelial cells were identified by their proximity to fractured profiles of melanosomes that had been inserted into the canal as a marker before freeze fracturing (Fig. 1). Schlemm's canal endothelial cells were joined by continuous zonulae occludentes. The complexity of these junctions varied along their length. The tight junctions between endothelial cells were categorized as representing either a single tight junctional strand, two strands, or three or more strands (Fig. 2). Only in their most complex form was the branching and anastomosing pattern of typical tight junctions observed. The intramembranous particles of the junctions fractured preferentially

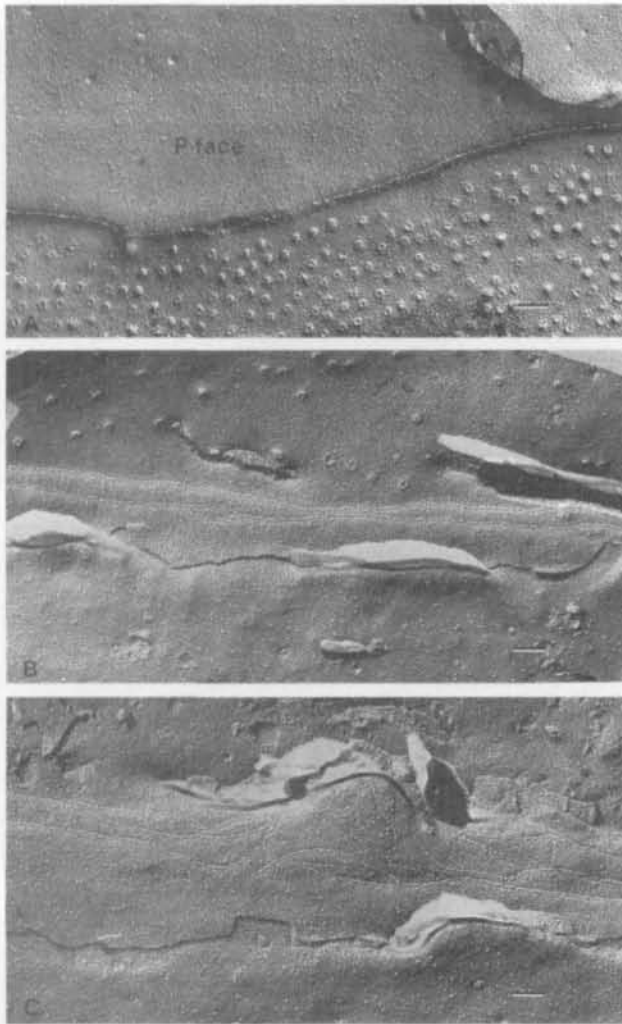


**FIGURE 2.** The tight junctions between endothelial cells were categorized as representing either a single tight junctional strand (A), two strands (B), or three or more strands (C). Magnification scale bar = 0.2  $\mu\text{m}$ .

with the E-face, where they were positioned at the base of shallow valleys. On the P-face, shallow ridges with a few particles at their crests were observed.

The general characteristics of the junctions between endothelial cells at each perfusion pressure were similar to those observed after immersion fixation. Although all three categories of junctional strand complexity were found in all eyes, regardless of fixation pressure, the intercellular junctions of the endothelial cells of SC fixed under pressure were less complex than those fixed by immersion. The morphometric data are summarized in Table 1.

With increasing perfusion pressure, the percentage of the total length of the junctions represented by three or more strands was reduced from 24.17% at 0 mm Hg to 8.59% at 45 mm Hg ( $P < 0.0012$ , line from linear regression [ $R^2 = 0.669$ ]; Fig. 3). Conversely, the percentage of the total length of the junc-

**TABLE 1.** Complexity of Total Junctional Length (%)

Pressure (mm Hg)	1 Strand	2 Strands	$\geq 3$ Strands
0	39.40 $\pm$ 11.00	36.43 $\pm$ 7.56	24.17 $\pm$ 9.41
15	47.56 $\pm$ 10.50	34.38 $\pm$ 5.47	18.06 $\pm$ 6.09
45	61.53 $\pm$ 6.58	29.88 $\pm$ 6.12	8.59 $\pm$ 1.33

Values are mean  $\pm$  SD (%);  $n = 4$ .

tions represented by one strand increased from 39.40% at 0 mm Hg to 61.53% at 45 mm Hg. The data for eyes perfused at 15 mm Hg fell between these two extremes.

In several instances, a fortuitous fracture plane cut through the lumen of a giant vacuole (Fig. 4). The membrane surrounding the opening exhibited tight junctions along one side of the vacuole. The membrane bleb produced by the vacuole distorted the rectilinear course of the tight junction and prompted a focal reduction in junction complexity as compared with the undistorted regions of the membrane adjacent to the vacuole (see Fig. 4). Invariably, the portion of the junction in the area of the membrane distorted by the vacuole had less complex junctions than in the adjacent undistorted area.

### Thin Sections

In thin sections from immersion-fixed specimens, substantial overlap between adjacent endothelial cells of SC was commonly observed. The average length of cell overlap was 0.63  $\mu\text{m}$ . Giant vacuoles were rarely seen (Fig. 5). At perfusion pressures of 15 and 45 mm Hg, giant vacuoles were evident (Figs. 5 and 6). Adjacent endothelial cells continued to overlap, but the amount

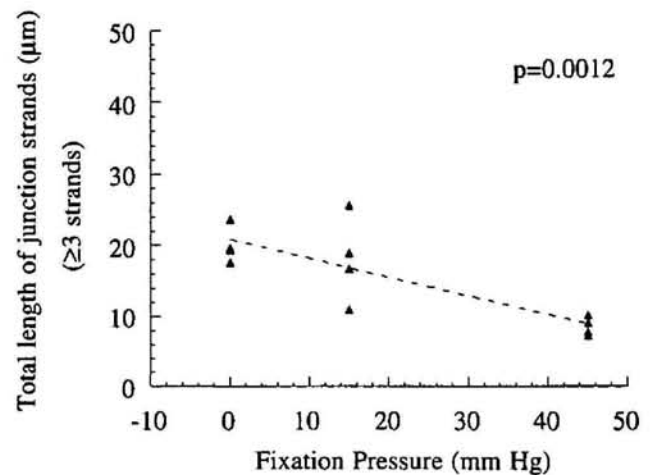


**FIGURE 3.** As the perfusion pressure increased, the percentage of the total length of junctions with three or more strands decreased ( $P < 0.0012$ ).

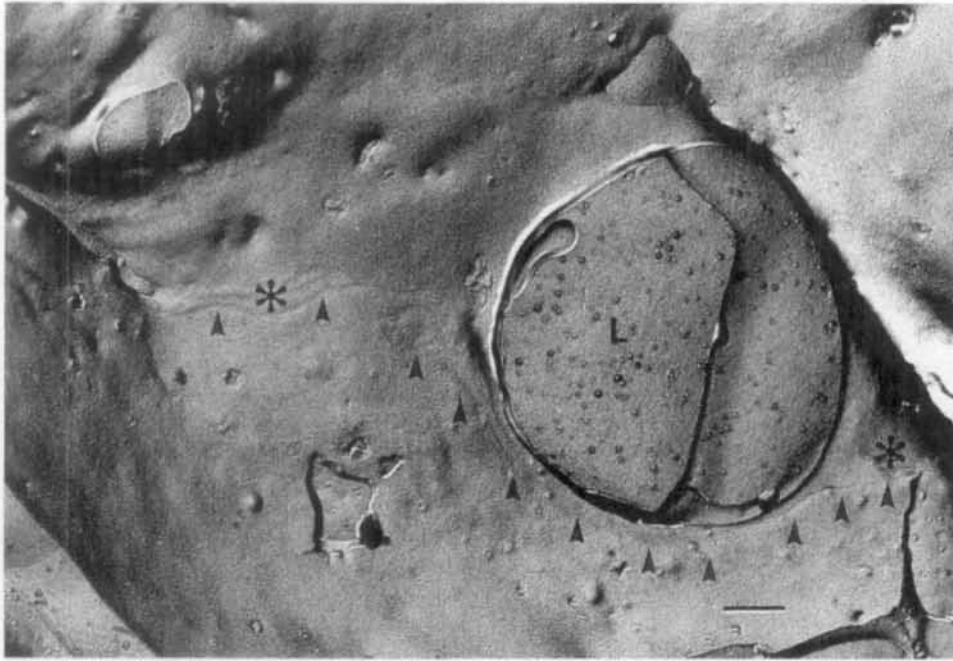


**FIGURE 4.** Rarely, the fracture plane cut through the lumen of a giant vacuole (L). The resulting distention of the endothelial cell membranes diverted the course of the interendothelial junction joining the two cells involved (*arrowheads*). In the distended area of the membrane, substantial simplification of junctional structure was evident. Areas of the junction on either side of the distended area of the membrane continued to exhibit a more complex, multistranded junctional architecture (\*). Magnification scale bar = 0.5  $\mu\text{m}$  (perfusion pressure = 15 mm).

of the endothelial overlap was significantly less than in the immersion-fixed specimens ( $P < 0.02$ ; Table 2). In some areas, the adjacent cells barely touched one another and the length of interendothelial cleft was reduced to essentially zero, but there was no apparent separation, as would be seen at a pore (Fig. 7). Examination of serial sections revealed that several giant vacuoles were formed between adjacent endothelial cells,

indicating that there is a paracellular cleft in the wall of some giant vacuoles (Fig. 8). Pores could be seen either at the apices of vacuoles or at the junction between neighboring cells (Fig. 9). Some vacuoles showed more than one pore. Some cells were found to have an opening on the side of the juxtacanalicular tissue in one plane of section and another opening on the

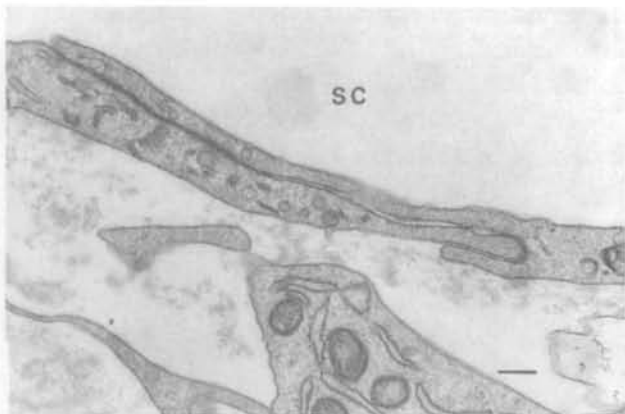


**FIGURE 5.** In thin sections from immersion-fixed eyes, extensive endothelial cell overlap is evident. No giant vacuoles are seen. Magnification scale bar = 0.2  $\mu\text{m}$ . SC: Schlemm's canal.

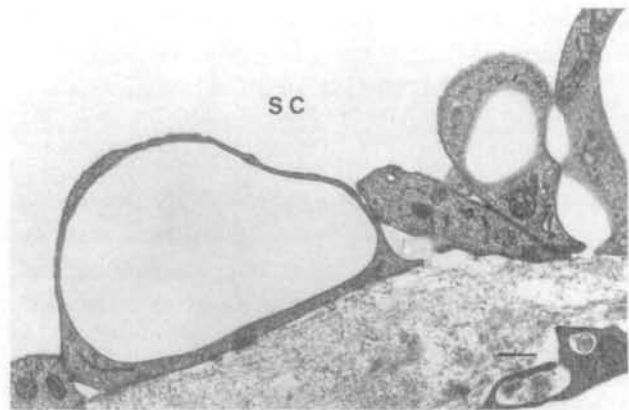


**FIGURE 6.** In thin sections of an eye fixed at 15 mm Hg, endothelial cell overlap was still seen but overlap was less than in immersion-fixed specimens. Giant vacuoles can be seen between endothelial cells of the inner wall of Schlemm's canal (SC). Magnification scale bar = 0.4  $\mu\text{m}$ .

TABLE 2. Change in Cell Overlap With Pressure

Pressure (mm Hg)	Age (years)	Number of Cells Measured	Average Cell Overlap ( $\mu\text{m}$ )	Mean $\pm$ SD
45	72	100	0.51	0.33 $\pm$ 0.13
	81	128	0.35	
	61	141	0.23	
	70	109	0.24	
15	72	113	0.29	0.34 $\pm$ 0.12
	81	134	0.27	
	61	193	0.28	
	70	102	0.51	
0	89	108	0.63	0.63 $\pm$ 0.08
	81	100	0.74	
	64	101	0.56	
	78	114	0.60	

Difference between 0 and 15 mm ( $P < 0.01$ ). Difference between 0 and 45 mm ( $P < 0.02$ ). No difference between 15 and 45 mm ( $P < 0.9$ ).

side of SC in an adjacent plane of section. In addition, paracellular lacunae were seen, some forming direct communication between SC and the juxtacanalicular tissue, providing a conduit for particulate matter such as free melanosomes. These openings into SC did not involve vacuoles (see Fig. 9).

#### Facility

The facility data for each eye and the relation to changes in the number of junctional strands are summarized in Table 3. Fixation led to a drop in facility ( $P < 2 \times 10^{-5}$ ). The mean ratio of facility after fixation compared with before fixation was 0.37. The Spearman correlation coefficient between facility before and after fixation was 0.47. There was no statistically

significant relation between facility and number of junctional strands.

#### DISCUSSION

In our study, we used freeze fracture and serial thin sections to examine intercellular junctions between the endothelial cells in SC of normal human eyes fixed at various pressures (0, 15, and 45 mm Hg). Specifically, we studied the changes in the amount of endothelial cell overlap and the numbers of junctional strands in perfusion-fixed versus immersion-fixed eyes. We found a reduction in endothelial cell overlap in perfusion-fixed eyes and documented statistically significant reductions in junctional complexity with increasing pressure.

The changes we found in immersion-versus perfusion-fixed eyes are unlikely to be caused by changes that developed in the 24-hour postmortem period. In our previous studies of junctions in the inner wall of SC in human eyes fixed by immersion, the structure of the junctions, as seen by freeze fracture, was remarkably similar to the junctions described between inner-wall cells of monkey eyes sacrificed immediately before fixation.<sup>7,9</sup>

Our results show that the number of strands and the complexity of the tight junctions between inner-wall endothelial cells decreased with increasing pressure. These data indicate that these intercellular junctions, like tight junctions in other systems,<sup>15</sup> are labile and responsive to changing physiological conditions. The physiological function of this simplification is not yet known. It may relate to the response of the intracellular cytoskeletal matrix to the altered stress distribution, or it could be related to the process of inner-wall

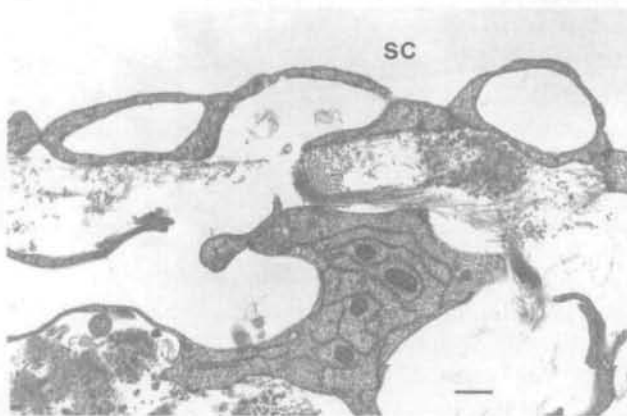


FIGURE 7. In thin sections of an eye fixed at 45 mm Hg, giant vacuoles are seen and the amount of endothelial cell overlap is reduced. Some of the endothelial cells barely contact each other. Magnification scale bar = 0.4  $\mu\text{m}$ . SC: Schlemm's canal.

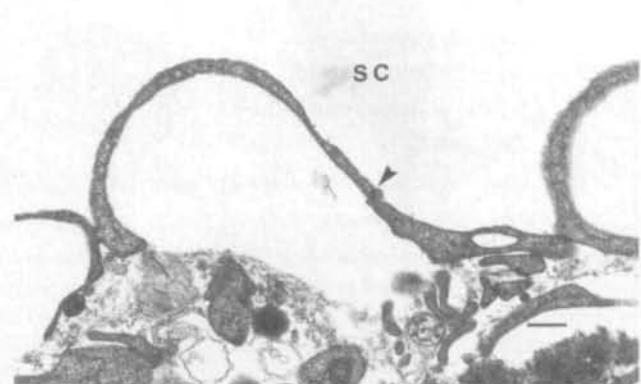
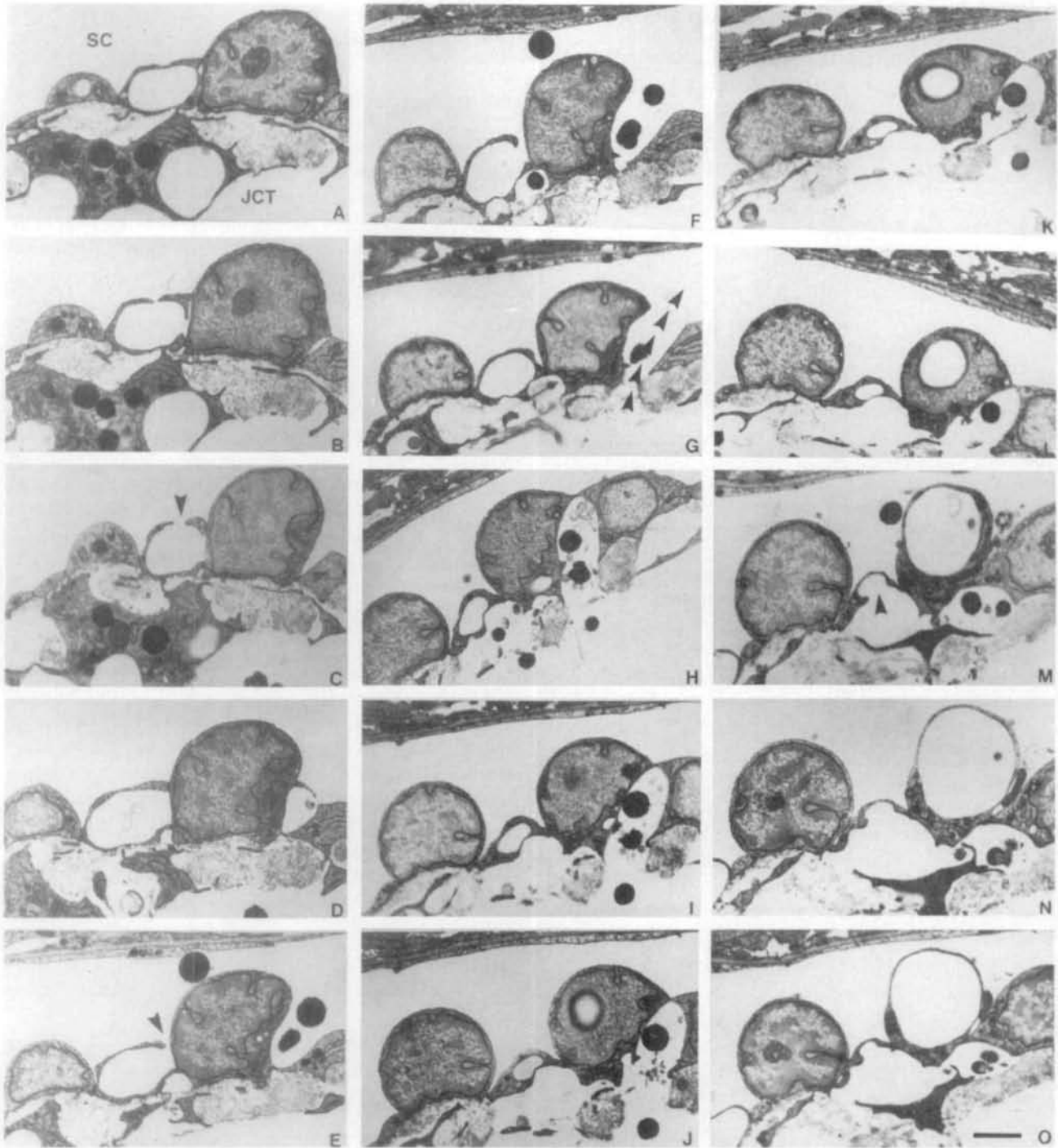


FIGURE 8. In thin sections, vacuoles were commonly formed between two adjacent endothelial cells. This example, fixed at 45 mm Hg, shows a junction at a position in the wall of the vacuole that is consistent with the position of the junction shown in Figure 4 (arrowhead). Magnification scale bar = 0.5  $\mu\text{m}$ . SC: Schlemm's canal.



**FIGURE 9.** Serial sectioning shows that giant vacuoles are formed both intra- and interendothelially. (C) An intracellular pore at the top of a vacuole (*arrowhead*). (E) A pore at the junction of two inner-wall cells. (G) An opening from the juxtacanalicular tissue (JCT) to Schlemm's canal (SC; *arrowheads*) between two inner-wall cells. Compare this with the same opening at different planes of sections in A, B, C, D, E, and F. (M) An opening to the JCT at the base of a vacuole in the inner-wall cell (*arrowhead*). This is the same cell seen in C and E, where the pores are at different locations. (J, K, L, M, N, O) A vacuole at different planes of section in the inner-wall cell. (Magnification scale bar = 1  $\mu\text{m}$ .)

TABLE 3. Tight Junction Complexity and Facility (C)

Pressure (mm Hg)	Age (years)	Junction Strands (%)			C Value	
		1	2	>3	Prefixation	Postfixation
45	72	65.06	27.71	7.23	0.29	0.077
	81	51.87	39.00	9.13	0.21	0.079
	61	66.23	25.98	7.79	0.23	0.093
	70	62.96	26.85	10.19	0.199	0.025
15	72	35.78	38.53	25.69	0.19	0.064
	81	41.73	39.37	18.90	0.16	0.079
	61	55.20	28.10	16.70	0.24	0.105
	70	57.53	31.51	10.96	0.259	0.131
0	89	53.93	26.70	19.37	—	—
	81	39.53	41.09	19.38	—	—
	64	36.81	43.56	19.63	—	—
	77	27.34	34.38	38.28	—	—

pore formation, which is also known to be pressure-sensitive.<sup>14</sup>

Several investigators have demonstrated that the permeability of epithelial and endothelial cell layers correlates well with the number and complexity of tight junctional strands as shown by freeze fracture.<sup>17,18</sup> In addition, we previously demonstrated that the increased blood–aqueous barrier permeability that attends anterior uveitis is reflected principally in barrier junction simplification rather than complete dissolution.<sup>19,20</sup> As such, it is reasonable to predict that the progressive junctional simplification we have seen should lead to enhanced flow across the inner wall of SC by the paracellular route.

It is clear from the sectioned material that some particulate matter, and therefore some aqueous, crosses into SC through focal separations between endothelial cells. Obviously, at these points, the number of junctional strands has been reduced to zero. Having pores form through a focal reduction in the junctional strand number to zero, whether within the wall of a giant vacuole or not, would seem to offer distinct biologic advantages. In vitro models of junction reassembly document that reestablishment of junctional integrity after focal disruption is rapid and is dependent on neither energy nor protein synthesis.<sup>21</sup> This nondependence on energy is entirely consistent with the accepted view that vacuole and pore formation (and thus aqueous outflow) is not energy-dependent. Unfortunately, focal reductions in strand number to zero are exceedingly difficult to document using freeze fracture, given the arbitrary nature of the fracture plane through the tissue.

The lack of correlation of outflow facility with the number of junctional strands could be caused by the small sample size. Nonetheless, the data show a trend that seems to favor a relation (e.g., at both pressures, the highest C value is also in the specimen with the

lowest percentage of three strands), but statistical significance has not been established. It is more difficult to assess what correlation might exist between facility and the focal interruptions in these junctions or to quantify the amount of increased flow that would attend the junctional simplification.

Epstein and Rohen,<sup>5</sup> using cationized ferritin perfusion, reported that the tight junctions between inner-wall cells could form openings or lacunae with tunnellike channels between the cells. Lacunae were evident in our sectioned material as well. The present studies reveal that the intercellular junction between two cells is not a static structure. The fact that blood corpuscles and macrophages (and in the present studies melanosomes) are occasionally seen in the lacunae during perfusion fixation<sup>22</sup> also supports the notion that inner-wall intercellular junctions are dynamic structures under physiological conditions.

In the present studies, freeze fracture showed a cross-fractured vacuole surrounded by tight junctions on one side, with junctional simplification in the area of the vacuole (see Fig. 4). In thin sections, several giant vacuoles were observed to be formed by two or more adjacent cells (see Fig. 8). When the junction was located toward one side of the vacuole near its base, the morphology is consistent with observations in freeze fracture. These results are in agreement with earlier reports that a certain number of “giant vacuoles” appear to be pseudovacuaes—that is, they are not all intracellular.<sup>5,23,24</sup>

The current consensus is that the bulk outflow of aqueous humor across the inner wall of SC passes into the giant vacuoles and through the pores.<sup>3,25</sup> However, this event may involve both transcellular and paracellular routes, because in previous studies<sup>5,23,24</sup> and in our study, at least some giant vacuoles were seen to be formed by the interdigitating processes of two or more adjacent endothelial cells.

Our study shows that the paracellular route across SC is pressure-sensitive and may respond to altered flow conditions. Further experiments will be necessary to evaluate the extent to which aqueous humor flow passes through paracellular channels in the inner-wall endothelium. The simplification of intercellular junctions that occurs as intraocular pressure increases may be related to the process of paracellular channel formation or the formation of pores, when pores are formed between cells rather than through them. It will be interesting to investigate this phenomenon in human glaucomatous eyes.

#### Acknowledgment

The authors thank Rozanne Richman, M.S., for excellent technical assistance.

#### References

- Garron LK, Feeney ML, Hogan MJ, McEwen WK. Electron microscopic studies of the human eye. *Am J Ophthalmol.* 1958;40:27-35.
- Holmberg A. The fine structure of the inner wall of Schlemm's canal. *Arch Ophthalmol.* 1959;62:956-958.
- Tripathi RC. Ultrastructure of Schlemm's canal in relation to aqueous outflow. *Exp Eye Res.* 1968;7:335-341.
- Bill A, Svedbergh B. Scanning electron microscopic studies of the trabecular meshwork and the canal of Schlemm: An attempt to locate the main resistance to outflow of aqueous humor in man. *Acta Ophthalmol.* 1972;50:295-320.
- Epstein DL, Rohen JW. Morphology of the trabecular meshwork and inner-wall endothelium after cationized ferritin perfusion in the monkey eye. *Invest Ophthalmol Vis Sci.* 1991;32(1):160-171.
- Ethier CR, Sit AJ, Coloma FM, Johnson M: Two populations of pores of the inner wall endothelium of Schlemm's canal. *Invest Ophthalmol Vis Sci.* (In press).
- Raviola G, Raviola E. Paracellular route of aqueous outflow in the trabecular meshwork and canal of Schlemm. *Invest Ophthalmol Vis Sci.* 1981;21(part 1):52-72.
- Okinami S, Matsumura M, Ohkuma M. Freeze-fractured replica of Schlemm's canal and the trabecular meshwork in the primate. *Graefes Arch Clin Exp Ophthalmol.* 1981;217:17-26.
- Bhatt K, Gong H, Freddo T. Freeze-fracture studies of interendothelial junctions in the angle of the human eye. *Invest Ophthalmol Vis Sci.* 1995;36:1379-1389.
- Johnston MA, Grant WM. Pressure-dependent changes in structures of the aqueous outflow system of human and monkey eyes. *Am J Ophthalmol.* 1973;75:365-383.
- Moses RA. The effect of intraocular pressure on resistance to outflow. *Surv Ophthalmol.* 1977;22:88-100.
- Grierson I, Lee WR. The fine structure of the trabecular meshwork at graded levels of intraocular pressure. 1. Pressure effects within the near-physiological range (8-30 mm Hg). *Exp Eye Res.* 1975;20:505-521.
- Grierson I, Lee WR. The fine structure of the trabecular meshwork at graded levels of intraocular pressure. 2. Pressure outside the physiological range (0 and 50 mm Hg). *Exp Eye Res.* 1975;20:523-530.
- Grierson I, Lee WR. Pressure-induced changes in the ultrastructure of the endothelium lining Schlemm's canal. *Am J Ophthalmol.* 1975;80:863-884.
- Ohnishi Y, Tanaka M. Effects of pilocarpine and paracentesis on occluding junctions between the nonpigmented ciliary epithelial cells. *Exp Eye Res.* 1981;32:635-647.
- Whale MD, Grodzinsky AJ, Johnson M. The effect of aging and pressure on the specific hydraulic conductivity of the aortic wall. *Biorheology.* 1996;33:17-44.
- Claude P, Goodenough D. Fracture faces of zonulae occludentes from "tight" and "leaky" epithelia. *J Cell Biol.* 1973;58:390-400.
- Claude P. Morphological factors influencing transepithelial permeability: A model for the resistance of the zonula occludens. *J Membr Biol.* 1978;39:219-232.
- Freddo TF. Intercellular junctions of the ciliary epithelium in anterior uveitis. *Invest Ophthalmol Vis Sci.* 1987;28:320-329.
- Freddo TF, Sacks-Wilner R. Interendothelial junctions of the rabbit iris vasculature in anterior uveitis. *Invest Ophthalmol Vis Sci.* 1989;30:1104-1111.
- Meldolesi J, Castiglioni G, Parma R, Nassivera N, DeCamilli P. Ca<sup>++</sup> dependent disassembly and reassembly of occluding junctions in guinea pig pancreatic acinar cells. Effect of drugs. *J Cell Biol.* 1978;79:156-172.
- Tripathi RC. Mechanism of the aqueous outflow across the trabecular wall of Schlemm's canal. *Exp Eye Res.* 1971;11:116-121.
- Fink AI, Felix MD, Fletcher RC. Schlemm's canal and adjacent structures in glaucomatous patients. *Am J Ophthalmol.* 1972;74:893-906.
- Grierson I, Johnson NF. The post-mortem vacuoles of Schlemm's canal. *Graefes Archiv Ophthalmologie* 1981;215:249-264.
- Tripathi RC. The functional morphology of the outflow systems of ocular and cerebrospinal fluids. *Exp Eye Res.* 1977;25(suppl):65-116.